The effective-medium theory of magnetoplasma superlattices

1995 J. Phys.: Condens. Matter 7 315

(http://iopscience.iop.org/0953-8984/7/2/009)

J. Phys.: Condens. Matter 7 (1995) 315–326. Printed in the UK

The effective-medium theory of magnetoplasma superlattices

F G Elmzughi†‡, N C Constantinou† and D R Tilley†§

† Department of Physics, University of Essex, Colchester CO4 3SQ, UK
‡ Physics Department, Al-Fatah University, Post Box 13540, Tripoli, Libya
§ School of Physics, Universiti Sains Malaysia, 11800 USM, Penang, Malaysia

Received 22 July 1994, in final form 12 October 1994

Abstract. The expression for the effective-medium dielectric tensor of a superlattice in which the dielectric tensors of the constituent media are taken in general form (all elements non-zero) is employed to describe a plasma/non-plasma, e.g. doped/undoped semiconductor superlattice in a magnetic field B_0 at an arbitrary angle to the interface. The properties of surface polaritons are discussed in detail for the perpendicular (B_0 normal to interfaces) and Faraday (B_0 parallel to interfaces, propagation vector along B_0) configurations.

1. Introduction

The properties of collective excitations in superlattices have been a subject of increasing interest in recent years. The equations for optical propagation in a superlattice of alternating layers of dielectric media have been known since the work of Rytov (1955). More recent developments are reviewed by Raj and Tilley (1989).

It was realised later (Yariv and Yeh 1977, Raj and Tilley 1985), that in the far infrared the fact that the wavelength λ is much greater than the superlattice period D means that the superlattice behaves like an anisotropic bulk medium. The same result was obtained by Agranovich and Kravstov (1985) and Liu *et al* (1985) using a simple physical argument based on the continuity of the tangential components of the electric field $\boldsymbol{E}$ and the normal components of the displacement vector $\boldsymbol{D}$ across the superlattice interfaces. This effective-medium description has been applied extensively in far-infrared spectroscopy of semiconductor superlattices (Dumelow and Tilley 1993). In general it gives a good account of the data on long-period superlattices together with a clear physical interpretation of the various spectral features. In the absence of a magnetic field, the effective-medium approach has been applied (Perkowitz *et al* 1987, Dumelow *et al* 1991a, b) for analysis of experimental results on semiconductor superlattices in which one or both layers was doped. In this case the far-infrared response was due to the dielectric functions of the semiconductor, which included the contribution of the free carriers (plasma response), as well as the optic phonons. There should be advantages in extending work of this kind by the inclusion of an applied magnetic field, so that the permittivity of the doped layer takes a magnetoplasma form. Oliveros *et al* (1993), made a start by investigating the effective-medium approach in the Voigt configuration (the magnetic field parallel to the surface and perpendicular to the direction of the propagation). In this paper we give a more general discussion.

In section 2 we derive the form of the effective dielectric tensor for the general case when all elements may be non-vanishing. In section 3 the results of section 2 are used to study the magnetoplasma properties of a superlattice in a magnetic field perpendicular to the interfaces. Finally in section 4 the results are applied to the Faraday configuration (the magnetic field parallel to the surface and to the direction of propagation).

2. The effective dielectric tensor

We consider the geometry of figure 1, in which a magnetic field B_0 is applied at angle θ to the interface normal. For subsequent applications we take the tensor elements in the magnetoplasma form, but for the formal derivation we use the general expression

$$\varepsilon^{\alpha}(\omega) = \begin{pmatrix} \varepsilon^{\alpha}_{xx} & \varepsilon^{\alpha}_{xy} & \varepsilon^{\alpha}_{xz} \\ \varepsilon^{\alpha}_{yx} & \varepsilon^{\alpha}_{yy} & \varepsilon^{\alpha}_{yz} \\ \varepsilon^{\alpha}_{zx} & \varepsilon^{\alpha}_{zy} & \varepsilon^{\alpha}_{zz} \end{pmatrix} \tag{1}$$

where $\alpha = \mathrm{a}$ or b.

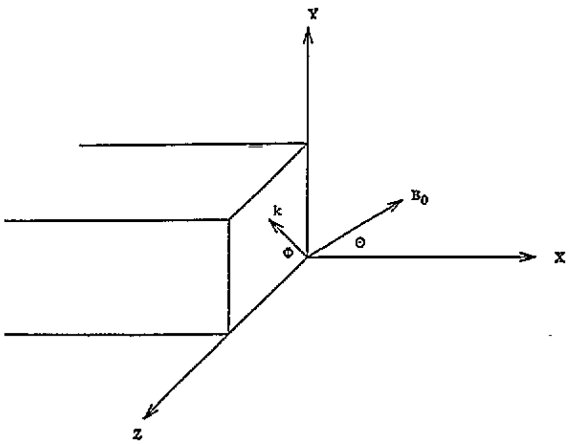

Figure 1. A magnetoplasma superlattice. Layers of thickness d_{a} and d_{b} alternate and a magnetic field is applied at angle θ to the interface normal.

We assume that the dielectric tensor at a point in the medium is independent of the distance of the point from the surface. This is a reasonable assumption for wavelengths much larger than the lattice spacing. Furthermore we neglect the wave-vector dependence of the dielectric tensor. In semiconductor problems this is generally satisfactory for excitations whose wavelength is large compared to the cyclotron orbit radius or to the carrier mean free path.

Following Agranovich and Kravstov (1985), Liu *et al* (1985) and Djafari Rouhani and Sapriel (1986) we argue that the field components E_y E_z and D_x are constant over many layers since they are continuous at the interfaces, whereas the other components are given by spatial averages over the values in each layer. Thus

$$\langle D_{y,z}\rangle = f_{\mathrm{a}} D^{\mathrm{a}}_{y,z} + f_{\mathrm{b}} D^{\mathrm{b}}_{y,z} \tag{2a}$$

$$\langle D_x\rangle = D^{\mathrm{a}}_x = D^{\mathrm{b}}_x \tag{2b}$$

$$\langle E_{y,z}\rangle = E^{\mathrm{a}}_{y,z} = E^{\mathrm{b}}_{y,z} \tag{2c}$$

and

$$\langle E_x \rangle = f_a E_x^a + f_b E_x^b \tag{2d}$$

where $f_a = d_a/(d_a + d_b)$ and $f_b = d_b/(d_a + d_b)$ are the volume fractions occupied by a and b. With use of

$$\boldsymbol{D} = \varepsilon(\omega) \cdot \boldsymbol{E} \tag{3}$$

straightforward algebra gives the effective dielectric tensor in the following general form:

$$\varepsilon(\omega) = \begin{pmatrix} \varepsilon_{xx} & \varepsilon_{xy} & \varepsilon_{xz} \\ \varepsilon_{yx} & \varepsilon_{yy} & \varepsilon_{yz} \\ \varepsilon_{zx} & \varepsilon_{zy} & \varepsilon_{zz} \end{pmatrix} \tag{4}$$

where

$$\varepsilon_{xx} = \varepsilon_{xx}^a \varepsilon_{xx}^b / (\varepsilon_{xx}^a f_b + \varepsilon_{xx}^b f_a) \tag{5a}$$

$$\varepsilon_{xy} = (\varepsilon_{xy}^a \varepsilon_{xx}^b f_a + \varepsilon_{xy}^b \varepsilon_{xx}^a f_b)/(\varepsilon_{xx}^a f_b + \varepsilon_{xx}^b f_a) \tag{5b}$$

$$\varepsilon_{xz} = (\varepsilon_{xz}^a \varepsilon_{xx}^b f_a + \varepsilon_{xz}^b \varepsilon_{xx}^a f_b)/(\varepsilon_{xx}^a f_b + \varepsilon_{xx}^b f_a) \tag{5c}$$

$$\varepsilon_{yx} = (\varepsilon_{yx}^a \varepsilon_{xx}^b f_a + \varepsilon_{yx}^b \varepsilon_{xx}^a f_b)/(\varepsilon_{xx}^a f_b + \varepsilon_{xx}^b f_a) \tag{5d}$$

$$\varepsilon_{yy} = \varepsilon_{yy}^a f_a + \varepsilon_{yy}^b f_b + f_a f_b (\varepsilon_{xy}^a - \varepsilon_{xy}^b)(\varepsilon_{yx}^b - \varepsilon_{yx}^a)/(\varepsilon_{xx}^a f_b + \varepsilon_{xx}^b f_a) \tag{5e}$$

$$\varepsilon_{yz} = \varepsilon_{yz}^a f_a + \varepsilon_{yz}^b f_b + f_a f_b (\varepsilon_{xz}^a - \varepsilon_{xz}^b)(\varepsilon_{yx}^b - \varepsilon_{yx}^a)/(\varepsilon_{xx}^a f_b + \varepsilon_{xx}^b f_a) \tag{5f}$$

$$\varepsilon_{zx} = (\varepsilon_{xx}^b \varepsilon_{zx}^a f_a + \varepsilon_{xx}^a \varepsilon_{zx}^b f_b)/(\varepsilon_{xx}^a f_b + \varepsilon_{xx}^b f_a) \tag{5g}$$

$$\varepsilon_{zy} = \varepsilon_{zy}^a f_a + \varepsilon_{zy}^b f_b + f_a f_b (\varepsilon_{xy}^a - \varepsilon_{xy}^b)(\varepsilon_{zx}^b - \varepsilon_{zx}^a)/(\varepsilon_{xx}^a f_b + \varepsilon_{xx}^b f_a) \tag{5h}$$

and

$$\varepsilon_{zz} = \varepsilon_{zz}^a f_a + \varepsilon_{zz}^b f_b + f_a f_b (\varepsilon_{xz}^a - \varepsilon_{xz}^b)(\varepsilon_{zx}^b - \varepsilon_{zx}^a)/(\varepsilon_{xx}^a f_b + \varepsilon_{xx}^b f_a). \tag{5i}$$

The above effective-medium tensor is a special case of the more general tensor recently obtained by Agranovich (1991).

In applications we concentrate on magnetoplasmas, for which a tensor rotation from a frame with z along $\boldsymbol{B}_0$ gives (Abdel-Shahid and Pakhomov 1970, Chiu and Quinn 1972, Wallis *et al* 1974)

$$\varepsilon^\alpha(\omega) = \begin{pmatrix} \varepsilon_1^\alpha \sin^2\theta + \varepsilon_3^\alpha \cos^2\theta & (\varepsilon_3^\alpha - \varepsilon_1^\alpha)\sin\theta\cos\theta & -\mathrm{i}\varepsilon_2^\alpha \sin\theta \\ (\varepsilon_3^\alpha - \varepsilon_1^\alpha)\sin\theta\cos\theta & \varepsilon_1^\alpha \cos^2\theta + \varepsilon_3^\alpha \sin^2\theta & \mathrm{i}\varepsilon_2^\alpha \cos\theta \\ \mathrm{i}\varepsilon_2^\alpha \sin\theta & -\mathrm{i}\varepsilon_2^\alpha \cos\theta & \varepsilon_1^\alpha \end{pmatrix} \tag{6}$$

where in numerical illustration we put

$$\varepsilon_1^\alpha = \varepsilon_\infty^\alpha \left(1 + \sum_j \frac{\omega_{pj}^{\alpha^2}}{(\omega_{cj}^{\alpha^2} - \omega^2)}\right) \tag{7a}$$

$$\varepsilon_2^\alpha = \varepsilon_\infty^\alpha \sum_j \frac{\omega_{cj}^\alpha \omega_{pj}^{\alpha^2}}{\omega(\omega^2 - \omega_{cj}^{\alpha^2})} \tag{7b}$$

and

$$\varepsilon_3^\alpha = \varepsilon_\infty^\alpha \left(1 - \sum_j \frac{\omega_{pj}^{\alpha^2}}{\omega^2}\right). \tag{7c}$$

Here the sums are over species of carrier indexed by j and ω_{cj}^α is the cyclotron frequency for layer α (a or b), defined by $\omega_{cj}^\alpha = eB_0/m_j^{*\alpha}$, where $m_j^{*\alpha}$ is the effective mass; ω_{pj}^α is the plasma frequency defined as $\omega_{pj}^{\alpha^2} = n_j^\alpha e^2/\varepsilon_\infty^\alpha m_j^{*\alpha}$, where $\varepsilon_\infty^\alpha$ is the background dielectric constant and n_j^α the carrier concentration. For simplicity we omit from (7) the optic-phonon contributions; this is satisfactory as long as ω_p and ω_c are not close to the phonon resonance frequencies (reststrahl region).

The expressions for the components of the effective-medium tensor for zero applied field, $\boldsymbol{B}_0 = \boldsymbol{0}$, are well known and have been extensively applied in discussion of the far-infrared optics of semiconductor superlattices (Dumelow and Tilley 1993, Dumelow *et al* 1993). Further, in the case of the Voigt configuration the relations have already been derived by Oliveros *et al* (1993). They give a full discussion of the implication for reflectivity, surface polaritons and attenuated total reflection.

Giuliani and Quinn (1983) first predicted intrasubband superlattice plasmon polaritons using the random-phase approximation (RPA) for strictly two-dimensional electron sheets. In the long-wavelength limit the Giuliani–Quinn dispersion relation can be derived classically via Maxwell's equations (see e.g. Constantinou and Cottam 1986). For well-width regimes such that a few subbands are occupied, classical methods break down and the full RPA treatment is required (see e.g. Bloss 1983). Finally, for wider well widths and at temperatures and doping levels such that very many subbands are occupied, the bulk form of the dielectric tensor is then valid. Backes *et al* (1992) have discussed this transition from two- to three-dimensional behaviour in detail and Bloss (1983) has made a comparison between the classical and quantum results. In all that follows we assume that any doped layer is wide enough so that a bulk plasma response is an adequate description; we therefore ignore any quantum-confinement effects.

3. The perpendicular configuration

Here we take $\boldsymbol{B}_0$ along the x axis, $\theta = 0$, so (4) becomes

$$\varepsilon(\omega) = \begin{pmatrix} \varepsilon_{xx} & 0 & 0 \\ 0 & \varepsilon_{yy} & \varepsilon_{yz} \\ 0 & \varepsilon_{zy} & \varepsilon_{zz} \end{pmatrix} \tag{8}$$

where

$$\varepsilon_{xx} = \varepsilon_3 = \varepsilon_3^a \varepsilon_3^b/(\varepsilon_3^a f_b + \varepsilon_3^b f_a) \tag{9a}$$

$$\varepsilon_{yy} = \varepsilon_{zz} = \varepsilon_1 = \varepsilon_1^a f_a + \varepsilon_1^b f_a \tag{9b}$$

and

$$\varepsilon_{yz} = -\varepsilon_{zy} = i\varepsilon_2 = i(\varepsilon_2^a f_a + \varepsilon_2^b f_b). \tag{9c}$$

The configuration has cylindrical symmetry about the external magnetic field, so the in-plane elements ε_{yy}, ε_{zz} and ε_{yz} are given by spatial averages of the corresponding elements of the two components, while the normal component ε_{xx} is the same as the parallel component in zero field.

The dispersion relation for bulk polaritons can be obtained directly from Maxwell's wave equation and takes the form

$$\varepsilon_3\beta^4 - (\varepsilon_1 k_3^2 + \varepsilon_3 k_1^2)\beta^2 + k_3^2(\varepsilon_1 k_1^2 + q_0^2\varepsilon_2^2) = 0. \tag{10}$$

Here we assume propagation in the (x, z) plane, $\boldsymbol{k} = (k_x, 0, k_z)$. Because the main interest is in surface polaritons we have put $k_x^2 = -\beta^2$, so that β will be the inverse decay length for a superlattice polariton. To simplify notation we put $k_z = k$ and define $k_i^2 = k^2 - q_0^2\varepsilon_i$ with $q_0 = \omega/c$. The solutions β_1 and β_2 of (10) for β^2 are given by

$$\beta^2 = k^2((\varepsilon_1 + \varepsilon_3)/2\varepsilon_3) - q_0^2\varepsilon_1 \pm [k^4((\varepsilon_1 - \varepsilon_3)/2\varepsilon_3)^2 - k_3^2 q_0^2 \varepsilon_2^2/\varepsilon_3]^{1/2}. \tag{11}$$

For a bulk material, $f_a = 1$ or $f_b = 1$, and (11) agrees with the corresponding result of Wallis *et al* (1974). Depending upon the position in the ω–k plane, the following possibilities may arise: (i) β_1 and β_2 are both real and positive, (ii) one is real and the other is pure imaginary, or vice versa, (iii) both are complex in which case they are conjugate or (iv) both are pure imaginary. Following established nomenclature (Wallis *et al* 1974), we classify the surface modes corresponding to these possibilities as (i) bonafide surface modes, (ii) pseudosurface modes, (iii) generalized surface modes and (iv) bulk (waveguide) modes. In all these cases (10) and (11) show that the medium is birefringent, i.e. there are two values of the wave vector $\boldsymbol{k}$ for a given frequency. As in all birefringent crystals (Landau and Lifshitz 1960), each of the two allowed modes has a definite polarization.

To derive the surface polariton dispersion relation, we write the fields in the two media (vacuum $x > 0$, and the effective medium $x < 0$), in the form

$$\boldsymbol{E}(r, t) = \boldsymbol{E}(x)\exp \mathrm{i}(kz - \omega t) \tag{12}$$

where

$$\boldsymbol{E}(x) = \boldsymbol{E}_0\,\mathrm{e}^{-\beta_0 x} \qquad \text{for } x > 0 \tag{13a}$$

and

$$\boldsymbol{E}(x) = \boldsymbol{E}_1\,\mathrm{e}^{-\beta_1 x} + \boldsymbol{E}_2\,\mathrm{e}^{-\beta_2 x} \qquad \text{for } x < 0. \tag{13b}$$

Here $\beta_0^2 = k^2 - q_0^2$ and β_1, β_2 are the two solutions of (11). There is a subtle difference between (13a) and (13b). As noted above, the effective medium is birefringent, with two possible values of β. Consequently the general solution of Maxwell's equations is a linear superposition of two terms, as written in (13b). In each term, however, the polarization is definite and therefore all the remaining field amplitudes are determined once a single one has been fixed. This means that there are just two unknowns in (13b), say E_{1y} and E_{2y}. On the other hand, (13a) relates to an isotropic medium, so the polarization is not definite. Therefore (13a) also includes two unknowns, say E_{0y} and E_{0z}; E_{0x} and the components of $\boldsymbol{H}$ are found in terms of these from Maxwell's equations.

The determination of the surface dispersion relation requires the matching of electromagnetic boundary conditions at $x = 0$, namely continuity of the tangential components of the electric and magnetic fields, E_y, E_z, H_y and H_z. Making use of

Maxwell's equations, we express the tangential components in terms of the unknowns E_{0y}, E_{0z}, E_{1y} and E_{2y}. The boundary conditions then yield the following dispersion relation:

$$(k_3^2\varepsilon_{\mathrm{m}}/\beta_0\varepsilon_3)[k_1^2+\beta_1\beta_2+\beta_0(\beta_1+\beta_2)]+\beta_1\beta_2(\beta_1+\beta_2)+\beta_0(\beta_1^2+\beta_1\beta_2+\beta_2^2)-\beta_0k_1^2=0. \tag{14}$$

This has the same form as was previously derived for the surface of a bulk medium (Wallis *et al* 1974, Chiu and Quinn 1972), because ε, equation (8), is formally identical to the bulk expression.

It is noted here that Kushwaha (1989, 1992) treated the effect of an applied magnetic field on the collective magnetoplasma excitations of semiconductor superlattices in the perpendicular configuration. These investigations were carried out in the framework of a transfer-matrix method. In the region of high frequency dispersion, which is that of most interest, the free-space wavelength is much greater than the superlattice period D (the effective-medium limit). This means that the wave number k appearing in the dispersion equations is small compared with D^{-1}. It is therefore possible to carry out systematic Taylor expansions to order k^2D^2 for those results in Kushwaha (1992) to drive (14).

In (14), k only appears in even powers, so the dispersion curves for positive and negative k are identical. That is, the surface-mode propagation is reciprocal, as required on symmetry grounds for the present case where the magnetic field is perpendicular to the surface (Camley 1987).

It is useful to find the expression for the non-retarded, or electrostatic, limit $k \gg q_0$, which is equivalent to $c \to \infty$. In this case the decay constants are given by

$$\beta_0=\beta_2=k \tag{15}$$

and

$$\beta_1=k(\varepsilon_1/\varepsilon_3)^{1/2}. \tag{16}$$

Equation (14) then reduces to

$$\varepsilon_3(\varepsilon_1/\varepsilon_3)^{1/2}=-1. \tag{17}$$

It follows from (16) and (17) that ε_1 and ε_3 must both be negative in order to have a bonafide surface mode in this limit, which means from (9) that ε_1^α and ε_3^α must be negative.

Typical results for surface-polariton dispersion curves are shown in figure 2 for the GaAs/AlAs system. In addition to the surface-mode curves we show the vacuum light line $\omega = ck$ and also one of the curves given by $\beta = 0$, which from (10) is seen to be equivalent to $k^2 = q_0^2\varepsilon_{\mathrm{V}}$, where $\varepsilon_{\mathrm{V}} = (\varepsilon_1^2 - \varepsilon_2^2)/\varepsilon_1$ is the Voigt permittivity. This is a boundary of the bulk continuum. In figure 2(*a*) $f_{\mathrm{a}} = 1.0$, corresponding to bulk GaAs. At low frequency a surface wave originates on the vacuum light line, then merges with the bulk continuum at $ck/\omega_{\mathrm{p}} \approx 1.3$. From $ck/\omega_{\mathrm{p}} \approx 1.3$ to $ck/\omega_{\mathrm{p}} \approx 3.9$ is a pseudosurface region (one β real and one pure imaginary); we did not follow the numerical solution through this region. The surface wave re-emerges from the bulk continuum at $ck/\omega_{\mathrm{p}} \approx 3.9$ and continues to the electrostatic limit, given by (17), as $k \to \infty$. The bounding frequencies of the pseudosurface-wave region can be found by solving (11) and (14) simultaneously with $\beta = 0$. This gives

$$\varepsilon_1(\varepsilon_{\mathrm{V}}-1)^{1/2}+(\varepsilon_{\mathrm{V}}(\varepsilon_1+\varepsilon_3)/\varepsilon_3-2\varepsilon_1)^{1/2}-\varepsilon_2^2/\varepsilon_1(\varepsilon_{\mathrm{V}}-1)^{1/2}=0 \tag{18}$$

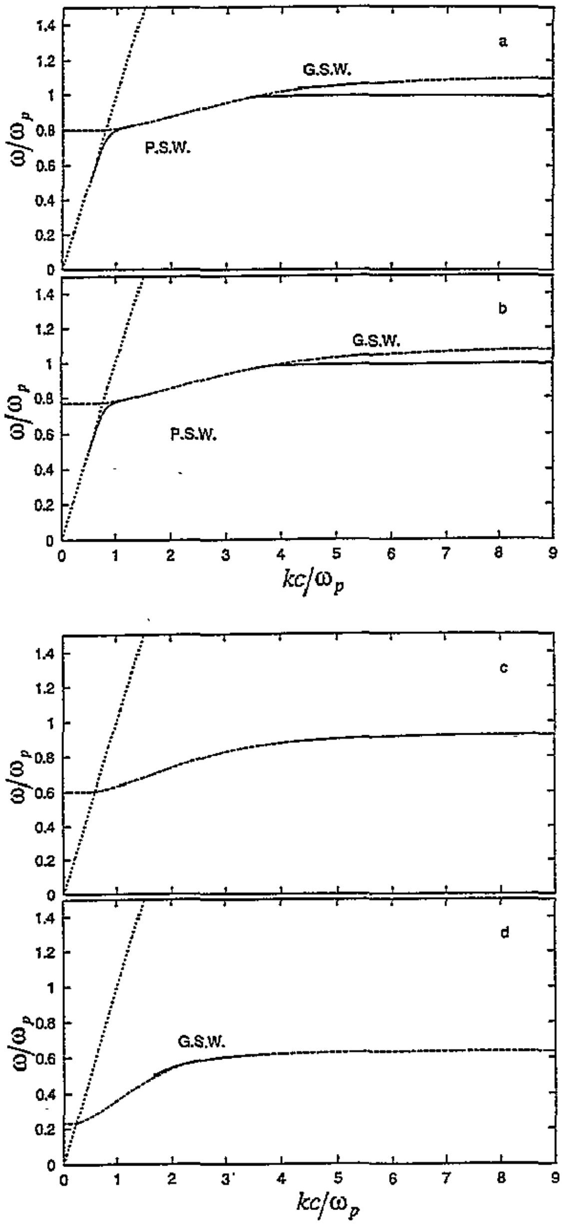

Figure 2. Surface-polariton dispersion curves ω versus k for GaAs (doped)/AlAs (undoped) with $\omega_c/\omega_p = 0.5$ and the field perpendicular to the surface. The high-frequency dielectric constants are $\varepsilon_\infty = 10.89$ (GaAs), $\varepsilon_\infty = 8.16$ (AlAs) (Adachi 1985). ——, surface and generalized surface waves; — — —, bulk continuum boundary ($\beta = 0$); ----, vacuum light line. (*a*) $f_a = 1$ (bulk GaAs), (*b*) $f_a = 0.9$, (*c*) $f_a = 0.5$, (*d*) $f_a = 0.1$.

which, apart from the third term on the left-hand side, agrees with the expression deduced by Wallis *et al* (1974).

At a higher frequency in the restricted wave-number range ck/ω_p between 4.3 and 5.9 we find a generalized surface wave (β_1 and β_2 both complex; roots taken with $\mathrm{Re}(\beta) > 0$)

just above the curve $k^2 = q_0^2\varepsilon_V$. These results are similar to those found by Wallis *et al* (1974) for bulk InSb.

Figure 2(*b*) corresponds to $f_a = 0.9$. The curves are similar to these for bulk GaAs (figure 2(*a*)) except that the lower-frequency surface-wave branch occupies a narrower range of k, as does the generalized surface wave. These branches continue to exist as long as $f_a > 0.5$. Figure 2(*c*) is for the critical value $f_a = 0.5$ at which the lower-frequency surface wave and the generalized surface wave just disappear and the higher-frequency surface wave just persists to the electrostatic limit. Finally, for $f_a < 0.5$ the surface wave is restricted to a finite range of ck/ω_p and takes on the character of a generalized surface wave. This is illustrated in figure 2(*d*) for $f_a = 0.1$.

The way in which the dispersion curves change with magnetic field is illustrated in figure 3, which is drawn for $f_a = 0.9$ so that comparison can be made with figure 2(*b*). Figures 2(*b*) and 3(*a*) show that for small enough B_0, i.e. small ω_c/ω_p, two surface-wave branches and a generalized surface wave are seen. The frequency interval occupied by the lower part of the surface wave decreases with increasing field. Numerical exploration shows that both surface-wave branches disappear at $\omega_c/\omega_p \approx 0.685$ and above this value of ω_c only the generalized surface wave appears. As comparison between figure 3(*a*)–(*d*) shows, the frequency of the generalized surface wave increases as ω_c increases. We also show in figure 3(*c*) and (*d*) the values of the real and imaginary parts of the complex-conjugate quantities β_1 and β_2 in the regions of the generalized surface wave. These are plotted as $\mathrm{Re}(\beta)/k$ and $\mathrm{Im}(\beta)/k$.

4. The Faraday configuration

The geometry with the applied magnetic field B_0 parallel to the direction of propagation, and therefore in the surface, is known as the Faraday configuration. In this case the effective dielectric tensor takes the form

$$\varepsilon(\omega) = \begin{pmatrix} \varepsilon_{xx} & \varepsilon_{xy} & 0 \\ \varepsilon_{yx} & \varepsilon_{yy} & 0 \\ 0 & 0 & \varepsilon_{zz} \end{pmatrix} \tag{19}$$

where

$$\varepsilon_{xx} = \varepsilon_1 = \varepsilon_1^a\varepsilon_1^b/(f_a\varepsilon_1^b + f_b\varepsilon_1^a) \tag{20a}$$

$$\varepsilon_{yy} = \varepsilon_2 = f_a\varepsilon_1^a + f_b\varepsilon_1^b - f_a f_b(\varepsilon_2^a - \varepsilon_2^b)^2/(f_a\varepsilon_1^b + f_b\varepsilon_1^a) \tag{20b}$$

$$\varepsilon_{xy} = -\varepsilon_{yx} = \mathrm{i}\varepsilon_T = (\varepsilon_1^b\varepsilon_2^a f_a + \varepsilon_1^a\varepsilon_2^b f_b)/(f_a\varepsilon_1^b + f_b\varepsilon_1^a) \tag{20c}$$

and

$$\varepsilon_{zz} = \varepsilon_3 = f_a\varepsilon_3^a + f_b\varepsilon_3^b. \tag{20d}$$

In this configuration the formal equations for the bulk and surface polaritons are similar to those for B_0 perpendicular to the surface. The equation that determines the decay constants β_i is

$$\varepsilon_2\beta^4 - (\varepsilon_2 k_1^2 + \varepsilon_3 k_2^2 + q_0^2\varepsilon_T)\beta^2 + \varepsilon_3(k_1^2k_2^2 - q_0^4\varepsilon_T^2) = 0 \tag{21}$$

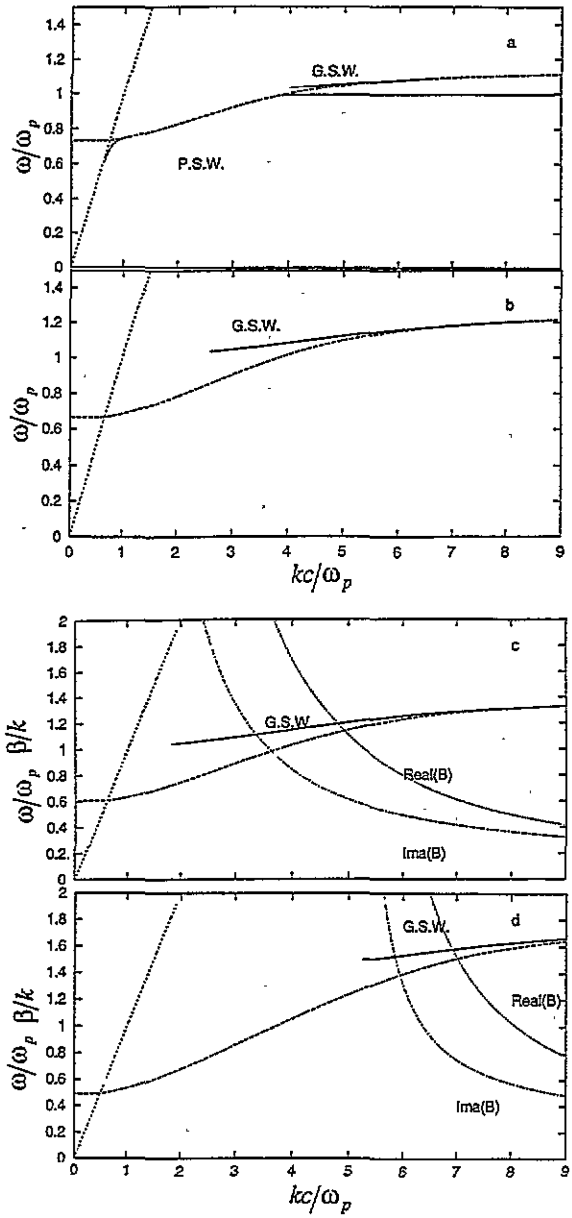

Figure 3. Surface-polariton dispersion curves ω versus k for GaAs (doped)/AlAs (undoped), with the field direction as in figure 2 and $f_a = 0.9$, and with (*a*) $\omega_c/\omega_p = 0.6$, (*b*) $\omega_c/\omega_p = 0.8$, (*c*) $\omega_c/\omega_p = 1.0$, (*d*) $\omega_c/\omega_p = 1.5$. (*c*) and (*d*) also show the curves for $\mathrm{Re}(\beta)/k$ (- - - -) and $\mathrm{Im}(\beta)/k$ (— · —) in the generalized surface wave.

with solutions

$$\beta^2 = (1/2\varepsilon_2)[(\varepsilon_2 k_1^2 + \varepsilon_3 k_2^2 + q_0^2\varepsilon_T^2) \pm ((\varepsilon_2 k_1^2 - \varepsilon_3 k_2^2 + q_0^2\varepsilon_T^2)^2 + 4k^2 q_0^2 \varepsilon_3 \varepsilon_T^2)^{1/2}]. \qquad (22)$$

For $f_a = 1.0$, (22) reduces to the corresponding result of Wallis *et al* (1974). The combinations of solutions of (22) may be classified, like those of (11), into surface, pseudosurface, generalized surface and bulk modes.

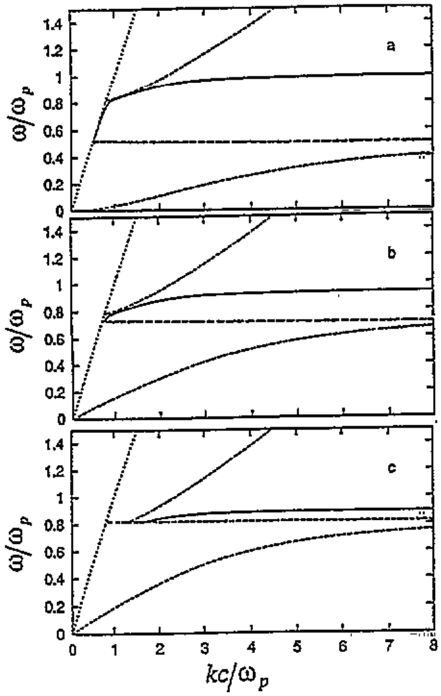

Figure 4. Surface-polariton dispersion curves ω versus k for GaAs (doped)/AlAs (undoped) in the Faraday configuration: the field is applied parallel to the interface with propagation along the field. Material parameters are as in figure 2, in particular $\omega_c/\omega_p = 0.5$. ——, surface and generalized surface waves; — — —, bulk continuum boundary; - - - -, vacuum light line. (*a*) $f_a = 1$ (bulk GaAs), (*b*) $f_a = 0.8$, (*c*) $f_a = 0.7$.

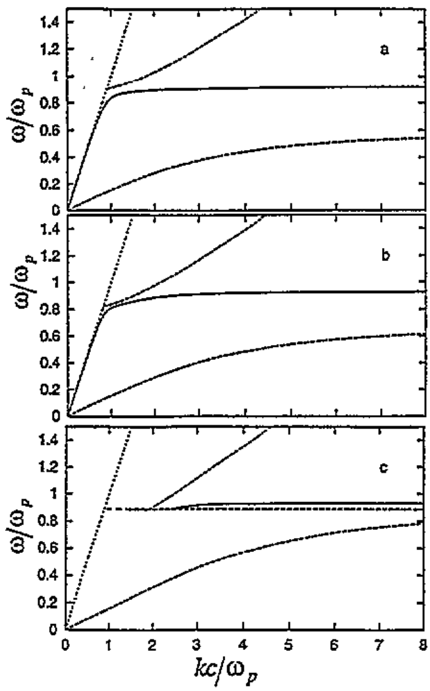

Figure 5. Surface-polariton dispersion curves ω versus k for GaAs (doped)/AlAs (undoped) with the field direction as in figure 4 and $f_a = 0.8$: (*a*) $\omega_c/\omega_p = 0.2$; (*b*) $\omega_c/\omega_p = 0.4$; (*c*) $\omega_c/\omega_p = 0.7$.

The derivation of the surface-mode dispersion relation follows that given in section 3 for the perpendicular configuration. The $\boldsymbol{E}$ fields in the two media are written in the form of (13) with independent variables E_{0y}, E_{0z}, E_{1y} and E_{2y}. Application of boundary conditions gives the following dispersion relation:

$$(\beta_0 + \beta_1 + \beta_2)\beta_1\beta_2\varepsilon_2 + [\beta_0(\beta_1 + \beta_2) + \beta_1^2 + \beta_1\beta_2 + \beta_2^2]\beta_0\varepsilon_2\varepsilon_3 + \beta_0 k_2^2 \varepsilon_3(1 - \varepsilon_2) = 0. \tag{23}$$

For $f_a = 1$ (23) reduces to the dispersion relation of Wallis *et al* (1974). As when $\boldsymbol{B}_0$ is perpendicular to the surface, k appears only in even powers in (23), so propagation is reciprocal, which is required by symmetry. In the non-retarded limit $k \gg q_0$ ($c \to \infty$) the decay constants are

$$\beta_0 = \beta_1 = k \tag{24}$$

and

$$\beta_2 = k(\varepsilon_3/\varepsilon_2)^{1/2} \tag{25}$$

with the surface-mode frequency given by

$$\varepsilon_2(\varepsilon_3/\varepsilon_2)^{1/2} = -1. \tag{26}$$

We have calculated numerical results for the same GaAs/AlAs system as in figures 2 and 3 and these are shown in figures 4 and 5. Bulk continuum regions are found by solving (21) with $\beta = 0$ and relevant boundary curves are shown in figures 4 and 5. The dispersion curve for the bulk material, $f_a = 1$, with $\omega_c/\omega_p = 0.5$ is shown in figure 4(*a*). The dispersion curve starts on the vacuum light line at $\omega = \omega_c$ and ultimately approaches the limiting non-retarded frequency. For $f_a < 1$ (figure 4(*b*) and (*c*)) the surface mode starts at the upper boundary of a bulk continuum rather than the light line.

Figure 5, drawn for $f_a = 0.8$ for comparison with figure 4(*b*), shows the way in which the dispersion curves depend on the magnetic field. Figure 5(*a*) and (*b*) corresponds to smaller fields (smaller ω_c/ω_p) than figure 4(*b*), while figure 5(*c*) corresponds to a larger field. It is seen that as the field value increases the frequency of the surface mode increases, corresponding to the increase in ω_c, and at the same time the frequency range (the difference between high-k and low-k frequencies) decreases. For small fields, figure 5(*a*) and (*b*), the dispersion curve starts on the vacuum light line, but for larger fields, figures 4(*b*) and 5(*c*), it starts at the top of the bulk continuum.

5. Conclusions

We have applied the general form of the effective-medium dielectric tensor to a magnetoplasma/isotropic superlattice with graphical results shown for the GaAs (doped)/AlAs (undoped) system. In order to focus on features that are specifically related to the magnetic field we have omitted reststrahl dispersion from the underlying dielectric constant. As mentioned in section 1, this is correct as long as the cyclotron and plasma frequencies ω_c and ω_p are sufficiently far from the TO and LO frequencies. If on the other hand, ω_c and ω_p are close to the reststrahl region then mode mixing of a well known kind occurs.

The main new results are the surface-polariton dispersion equations and curves for the perpendicular configuration (section 3) and the Faraday configuration (section 4). Compared with the Voigt configuration (Oliveros *et al* 1993) both these geometries suffer from the complication that the superlattice is birefringent. As discussed in section 3, this makes the derivation of the dispersion equation somewhat different. The superlattices support surface polariton-type modes in both these configurations, as well as in the Voigt configuration, and the general way in which the dispersion curves vary with magnetic field and with the volume fraction of the doped constituent is illustrated in sections 3 and 4.

The surface polaritons could be investigated by attenuated total reflection (ATR); an expression for the ATR reflectivity could be derived and computed without undue difficulty from the effective dielectric tensor. Substantial information about the dielectric tensor itself can be obtained by means of simpler techniques, for example oblique-incidence reflectivity (Dumelow *et al* 1993). Here again, relevant expressions could be derived in a straightforward way.

Acknowledgments

We are grateful for helpful discussion with Professor Rodney Loudon. FGE acknowledges financial support from Al-Fatah University and NCC financial support from the UK Science and Engineering Research Council.

References

Abdel-Shadid N C and Pakhomov V I 1970 *Plasma Phys.* **12** 55
Adachi S 1985 *J. Appl. Phys.* **58** R1
Agranovich V M 1991 *Solid State Commun.* **78** 747
Agranovich V M and Kravstov V E 1985 *Solid State Commun.* **55** 85
Backes W H, Peeters F M, Brosens F and Devrees J T 1992 *Phys. Rev.* B **45** 8437
Bloss W L 1983 *Solid State Commun.* **48** 927
Camley R E 1987 *Surf. Sci. Rep.* **7** 103
Chiu K W and Quinn J J 1972 *Phys. Rev.* B **5** 4707
Constantinou N C and Cottam M G 1986 *J. Phys. C: Solid State Phys.* **19** 739
Djafari Rouhani B and Sapriel J 1986 *Phys. Rev.* B **34** 7114
Dumelow T, Hamilton A A, Parker T J, Tilley D R, Samson B, Smith S R P, Beall R B and Harris J J 1991a *Superlatt. Microstruct.* **9** 517
Dumelow T, Parker T J, Smith S R P and Tilley D R 1993 *Surf. Sci. Rep.* **17** 151
Dumelow T, Parker T J, Tilley D R, Beall R B and Harris J J 1991b *Solid State Commun.* **77** 253
Dumelow T and Tilley D R 1993 *J. Opt. Soc. Am.* A **10** 633
Giuliani F and Quinn J J 1983 *Phys. Rev. Lett.* **51** 919
Kushwaha M S 1989 *Phys. Rev.* B **40** 1969
—— 1992 *Surf. Sci.* **262** 451
Landau L D and Lifshitz E M 1960 *Electrodynamics of Continuous Media* (Oxford: Pergamon)
Liu W, Eliasson G and Quinn J J 1985 *Solid State Commun.* **55** 533
Oliveros M C, Almeida N S and Tilley D R 1993 *Semicond. Sci. Technol.* **8** 441
Pakhomov V I and Stepanov K N 1967 *Zh. Tekh. Fiz.* **37** 1393 (Eng. transl. *Sov. Phys.–Tech. Phys.* **12** 1011 (1968))
Perkowitz S, Sudharsanan R, Harris K A, Cook J W Jr, Schulman J F and Schulman J N 1987 *Phys. Rev.* B **36** 9290
Raj N and Tilley D R 1985 *Solid State Commun.* **55** 373
—— 1989 *The Dielectric Function of Condensed Systems* ed L V Keldysh, D A Kirzhnitz and A A Maradudin (Amsterdam: Elsevier) ch 7
Rytov S M 1955 *Zh. Eksp. Teor. Fiz.* **29** 605 (Engl. transl. *Sov. Phys.–JETP* **6** 785)
Wallis R F, Brion J J, Burstein E and Hartstein A 1974 *Phys. Rev.* B **9** 3424
Yariv A and Yeh P 1977 *J. Opt. Soc. Am.* **67** 438